NHEJ, we measured sensitivity to ionizing radiation (IR) in the G_1 phase (Figure 3A and Supplementary Figure S5A). *SMARCAL1*$^{-/-}$ as well as *LIG4*$^{-/-/-}$ cells showed a hypersensitivity to IR (Figure 3B). As expected, the *SMARCAL1*$^{-/-}$/*LIG4*$^{-/-/-}$ cells showed the same hypersensitivity to IR as did the *LIG4*$^{-/-/-}$ cells in the G_1 phase (Figure 3B). We then monitored DSB repair kinetics in the G_1 phase by counting the number of γH2AX and 53BP1 foci over time after exposure to IR. The resolution of 53BP1 and γH2AX foci was significantly delayed in *SMARCAL1*$^{-/-}$ cells compared to *wild-type* cells (Figures 3C, D and Supplementary Figure S5B). These results indicate that *SMARCAL1*$^{-/-}$ cells are deficient in DSB repair in the G_1 phase. We therefore conclude that Smarcal1 promotes DSB repair by NHEJ in both human and chicken DT40 cells.

Deletion of Smarcal1 does not compromise the fidelity of NHEJ

To address the accuracy of individual DSB-repair events, we performed two experiments using TK6 cells, (i) the analysis of V(D)J recombination (Figure 4) and (ii) the repair of I-*Sce*1 induced DSBs by NHEJ (Figure 5).

V(D)J recombination is initiated by the Rag1 and Rag2 recombinase proteins, which introduce DSBs at the recombination signal (RS) (58,59) and complete recombination by collaborating with canonical NHEJ. We used two episomal V(D)J-recombination substrates, pJH200 and pJH290, where the recombinase generates the RS and coding-joint products, respectively (50) (Figure 4A). We transiently transfected expression plasmids encoding *RAG1* and *RAG2* along with either pJH200 or pJH290 into *wild-type* and *SMARCAL1*$^{-/-}$ and *LIG4*$^{-/-/-}$ cells (Figure 4B). We then recovered the transfected substrate plasmids from the TK6 cells, introduced the plasmids into bacterial cells, and plated them on LB agar plates containing either ampicillin or chloramphenicol. Ampicillin-resistant colonies contained recovered pJH200 or pJH290 plasmids, while colonies resistant to chloramphenicol contained only rearranged pJH200 or pJH290 plasmids. Thus, the frequency of rearrangement can be calculated as the gain of chloramphenicol-resistant (cam^R) colonies relative to the total number of ampicillin-resistant (amp^R) colonies. The signal-joint ends are precisely ligated, whereas the coding ends are joined in a process that can involve nucleotide loss or gain in addition to simple ligation (60). We failed to recover any rearranged signal-joint products from *LIG4*$^{-/-/-}$ cells, which agrees with the essential role for DNA Ligase4 in signal-joint formation (61,62). The efficiency of recombination in the signal-joint and coding-joint plasmids was decreased 2.3 and 2.4 times, respectively, in *SMARCAL1*$^{-/-}$ cells, when compared with *wild-type* cells (Figure 4C). The nucleotide sequence analysis of signal-joint products indicated that only a single product among the 29-analyzed sequences contained one nucleotide deletion in *SMARCAL1*$^{-/-}$ cells (data not shown). Analysis of coding joints, on the other hand, showed more frequent deletion events in *SMARCAL1*$^{-/-}$ as well as in *wild-type* cells, with the extent and frequency of deletion being comparable between the two genotypes (Supplemental Table S2). Thus, the loss of Smarcal1 reduces the efficiency of canonical NHEJ without compromising its fidelity.

We next examined individual DSB-repair events in the human TK6 cell line, which is heterozygous (+/-) for the thymidine kinase (*TK*) gene and contains an I-*Sce*1 endonuclease recognition site in the fourth intron of the intact *TK* allele (51) (Figure 5A). If the repair of I-*Sce*1-induced DSBs causes the deletion of more than 100 nucleotides downstream from the I-*Sce*1 site, the deletion would inactivate the fifth exon, leading to the formation of *TK*$^{-/-}$ cells, which cells are able to form colonies in the negative-selection media containing trifluorothymidine (TFT) (Figure 5A). We found that the number of TFT-resistant clones was reduced by 8 and 5 times in the *LIG4*$^{-/-/-}$ and *SMARCAL1*$^{-/-}$ cells, respectively, when compared with *wild-type* cells (Figure 5B). To analyze deletion range and pattern, we isolated at least 50 individual TFT-resistant clones from each genotype. Genomic PCR amplification over the I-*Sce*1 site indicated that deletion was two times shorter in the *SMARCAL1*$^{-/-}$ cells and approximately 0.5 times longer in *LIG4*$^{-/-/-}$ cells, compared with *wild-type* cells (Figure 5C and Supplementary Figure S6). In summary, we conclude that Smrcal1 promotes NHEJ without affecting its accuracy.

The RPA-binding domain and the ATPase domains are both required for the promotion of NHEJ by Smarcal1

The phenotypic analysis of *SMARCAL1*$^{\Delta 30/-}$ DT40 cells indicated that the RPA-binding site is essential for Smarcal1 to function in NHEJ. To confirm the relevance of this finding to human cells, we reconstituted the *SMARCAL1*$^{-/-}$ TK6 cells with the RPA-binding-site-deficient (*SMARCAL1*$^{\Delta 30}$) transgene as well as the *wild-type* (*SMARCAL1*^{WT}) transgene. The expression level of the Smarcal1 protein in the reconstituted cells was similar to that in the *wild-type* cells (Figure 5D, lower panel). As expected, reconstitution of *SMARCAL1*$^{-/-}$ cells with the *SMARCAL1*^{WT} transgene normalized the NHEJ-mediated repair of I-*Sce*1-induced DSBs (Figure 5E). The *SMARCAL1*$^{\Delta 30}$ transgene failed to normalize NHEJ, indicating that the RPA-binding site plays a role in promoting NHEJ by Smarcal1 in human cells. Moreover, *SMARCAL1*$^{-/-}$ cells and *SMARCAL1*$^{\Delta 30}$ transgene exhibited similar sensitivity to DNA-damaging agent (Supplementary Figure S4C), demonstrating that the RPA-binding site is critical for Smarcal1 DNA repair function. Next, to investigate the role of annealing helicase activity, we introduced a point mutation (Arginine 764 to Glutamine, R764Q) into the ATPase domain of the *SMARCAL1*^{WT} transgene, which mutation has no detectable annealing helicase activity (2) and causes a severe form of Schimke immuno-osseous dysplasia (SIOD) (4). Reconstitution with the resulting *SMARCAL1*^{R764Q} transgene did not restore the repair of I-*Sce*1-induced DSBs (Figure 5D and E). We therefore conclude that the annealing helicase activity as well as the physical association of Smarcal1 with RPA is required for the promotion of NHEJ by Smarcal1. One possible scenario is that Smarcal1 promotes NHEJ by interacting with unwound DSB ends associated with RPA and facilitate their annealing.

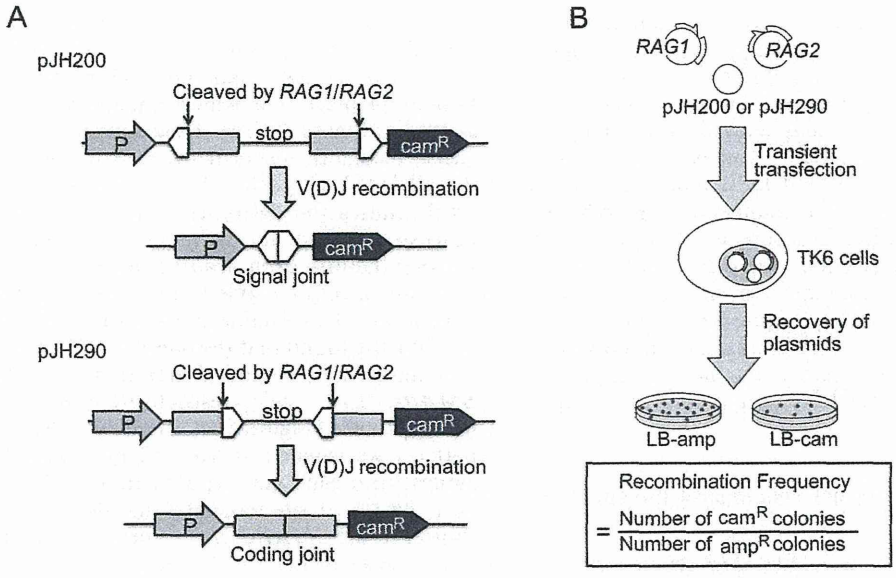

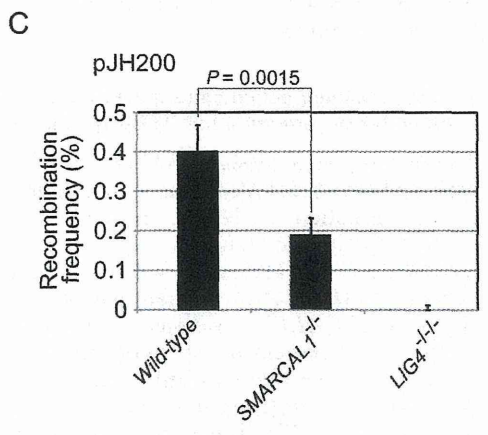

Cell lines	pJH200 (signal joint) camR/ ampR	Frequency (%)
Wild-type (Mock transfection)	0 / 26,523	0
Wild-type	90 / 22,720	0.40
SMARCAL1$^{-/-}$	29 / 15,420	0.19
LIG4$^{-/-/-}$	0 / 35,023	0

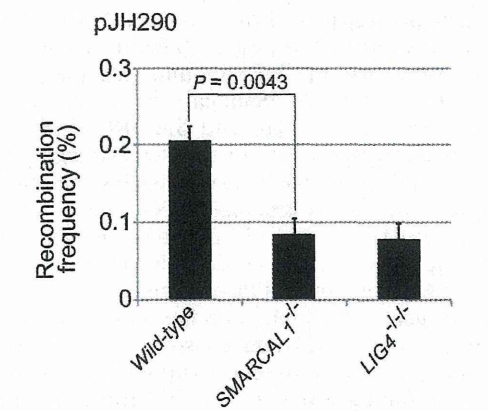

Cell lines	pJH290 (coding joint) camR/ ampR	Frequency (%)
Wild-type (Mock transfection)	0 / 22,540	0
Wild-type	17 / 8,261	0.21
SMARCAL1$^{-/-}$	21 / 24,721	0.085
LIG4$^{-/-/-}$	14 / 17,755	0.079

Figure 4. The loss of Smarcal1 reduces the efficiency of V(D)J recombination without compromising its fidelity. (**A**) The structure of two episomal V(D)J-recombination substrates, pJH200 and pJH290, and their recombination products. Open triangles and closed boxes represent recombination signals (RSs) and V(D)J-coding sequences, respectively. Cam^R = chloramphenicol-resistance gene; P = promoter. (**B**) Schematic representation of the experimental method for the V(D)J-recombination assay. Frequency of recombination was calculated by dividing the number of rearranged products (the number of cam^R colonies) by the number of recovered plasmids (the number of ampicillin-resistant [amp^R] colonies). (**C**) Recombination frequency of TK6 cells carrying the indicated genotypes. Data shown are the means of more than three experiments. Error bars indicate SD of more than three independent experiments. *P*-value was calculated by Student's *t*-test. The total number of ampicillin- and chloramphenicol-resistant colonies is shown in the right panel. Supplemental Table S2 shows the nucleotide sequences of coding joints associated with deletion events.

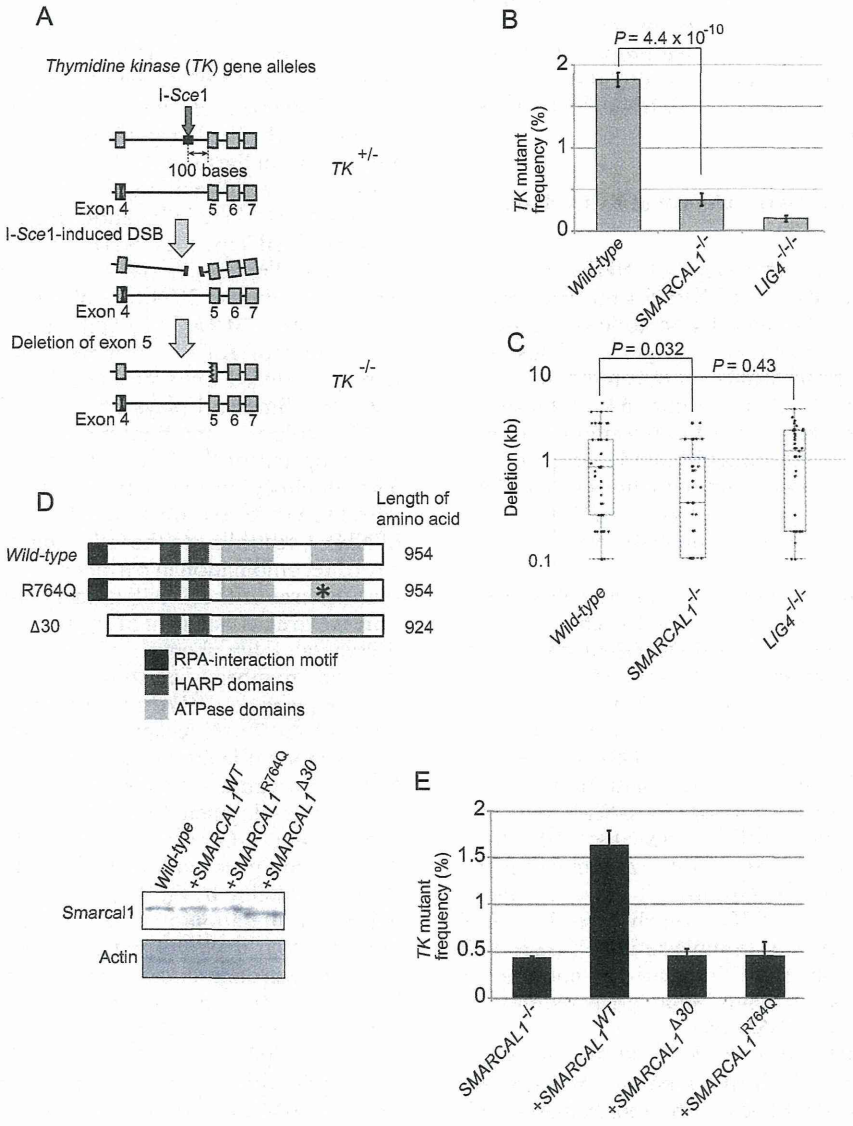

Figure 5. The fidelity of end-joining in *SMARCAL1* mutant cells. (**A**) Schematic diagram showing DSB-repair events that repair I-*Sce*1-induced DSBs in the endogenous thymidine kinase (*TK*) locus. $TK^{+/-}$ cells carry an I-*Sce*1 site in intronic sequences of the *wild-type TK* allele and a mutation in exon4 of the mutant *TK* allele. DSB repair associated with deletion in exon5 coding sequences would yield $TK^{-/-}$ clones from $TK^{+/-}$ cells. The number of $TK^{-/-}$ clones was measured by counting the number of trifluorothymidine (TFT)-resistant colonies. (**B**) Histogram representing the frequency of DSB-repair events (*y*-axis) in the indicated genotypes (*x*-axis). Error bars indicate SD of more than three independent experiments. *P*-value was calculated by Student's *t*-test. (**C**) Box plot representing the length of nucleotide deletion (*y*-axis) in the indicated genotypes (*x*-axis). PCR was performed from genomic DNA isolated from at least 50 TFT-resistant clones of each genotype, as shown in Supplementary Figure S6. (**D**) Schematic representation of the structure of *wild-type*, R764Q and Δ30 Smarcal1 proteins. $SMARCAL1^{-/-}$ TK6 cells were reconstituted with $SMARCAL1^{WT}$, $SMARCAL1^{\Delta 30}$ or $SMARCAL1^{R764Q}$ transgene. Western blot analysis for the expression of individual transgenes in $SMARCAL1^{-/-}$ cells. β-actin was used as a loading control. (**E**) Histogram representing the frequency of TFT-resistant colonies (*y*-axis) in the indicated genotypes (*x*-axis). Error bars indicate SD of more than three independent experiments.

Annealing of double-strand DNA by purified Smarcal1 (2) suggests that Smarcal1 facilitates NHEJ by stabilizing the physical interaction between Ku70/Ku80/DNA-PKcs proteins and DSB ends, thereby activating DNA-PKcs. To test this hypothesis, we analyzed the phosphorylation status of threonine 2609 (63,64) after treatment with the topoisomerase 2 inhibitors ICRF193 (Supplementary Figures S7A and S7B) and etoposide (Supplementary Figure S7C). Strikingly, the phosphorylated threonine 2609 was detectable only in the *wild-type* and not in the $SMARCAL1^{-/-}$ cells (Supplementary Figures S7B and S7C). The compromised phosphorylation of DNA-PKcs may account for the decreased efficiency of NHEJ, as the substitution of the threonine 2609 site to alanine

causes radio-sensitivity and reduced V(D)J recombination efficiency, which sensitivity is less prominent than that of *DNA-PKcs* null-mutant cells (64). We propose that Smarcal1 promotes NHEJ, presumably at an initial step, by facilitating the physical association of Ku70/Ku80/DNA-PKcs proteins and DSB ends.

Smarcal1 is required for the recruitment of XRCC4 to DNA-damage sites

To investigate early and late steps of NHEJ, we monitored the dynamics of Ku70 and XRCC4 proteins, respectively, in the chromatin-bound fraction, following exposure of cells to ICRF193 for one hour (Figure 6). This exposure did not affect the purification of the chromatin-bound or the nuclear-soluble fractions (Figure 6A). Exposure to ICRF193 caused a marked increase in the amounts of both Ku70 and XRCC4 in the chromatin-bound fraction of *wild-type* cells. In marked contrast, accumulations of Ku70 and XRCC4 in the *SMARCAL1*$^{-/-}$ as well as *DNA-PKcs*$^{-/-}$ cells were, significantly smaller compared with *wild-type* cells (Figure 6B and C).

To validate the significant reduction in the accumulation of XRCC4 near DSB sites, we conducted chromatin immunoprecipitation (ChIP) following transient transfection of empty vector and expression vectors encoding the I-*Sce*1 restriction enzyme and a TALEN towards the *p53* locus (Figure 6D). XRCC4 is supposed to accumulate at the *TK-I* or *p53-I* sites, which are adjacent to the DSB sites, but not at the *TK-II* or *p53-II* sites, which are distant from the DSB sites (Figure 6D). Transient expression of I-*Sce*1 or TALEN caused the accumulation of XRCC4 near the DSB sites in *wild-type* cells, whereas the extent of the accumulation was significantly reduced in *SMARCAL1*$^{-/-}$ cells (Figure 6E and Supplementary Figure S7D). We checked the overall expression levels of XRCC4 (Supplementary Figure S7B) to confirm that the deletion of Smarcal1 did not alter the level of protein expression. Thus, Smarcal1 is required for recruitment of XRCC4 to DSB sites.

Like reduced accumulation of Ku70 in the chromatin fraction (Figures 6B and C), the amounts of Ku70 and DNA-PKcs near the I-*Sce*1 site were approximately 30% smaller in *SMARCAL1*$^{-/-}$ cells in comparison with *wild-type* cells (Figures 6F and G). In summary, Smarcal1 may promote annealing of DSB ends, which stabilizes complex formation of Ku/DNA-PKcs at DSB sites and fully activates DNA-PKcs. The activation may enhance the recruitment of XRCC4 for the completion of DSB repair by canonical NHEJ.

DISCUSSION

We herein show that Smarcal1 significantly contributes to canonical NHEJ. Although the role of Smarcal1 during DNA replication has been well established (1,3,8–10,65), it has remained unclear whether Smarcal1 plays a role outside the S phase. We here reveal that Smarcal1 contributes to DSB repair by NHEJ during the G_1 phase. The role played by Smarcal1 in NHEJ is demonstrated by six points, as follows. First, the loss of Smarcal1 increases cellular sensitivity to ICRF193, which induces DSBs repair only by NHEJ and not by HR (17) (Figures 1B and 2B). Second, null-mutation of *KU70* is epistatic to *SMARCAL1*$^{\Delta 30}$ mutation in DT40 cells (Figure 1D) and null-mutation of *LIG4* is epistatic to *SMARCAL1* null-mutation in TK6 cells (Figure 2D), in terms of cellular tolerance to ICRF193. Third, the loss of Smarcal1 significantly reduces the efficiency of DSB repair in the G_1 phase in TK6 cells (Figure 3). Fourth, *SMARCAL1* null-mutation in TK6 cells significantly compromises V(D)J recombination (Figure 4) as well as I-*Sce*1-induced DSB repair by NHEJ (Figure 5). Fifth, *SMARCAL1* null-mutation impairs the phosphorylation of DNA-PKcs at threonine 2609 (Supplementary Figures S7B and S7C). Lastly, *SMARCAL1* null-mutation diminishes the accumulation of Ku70, DNA-PKcs and XRCC4 at DNA-damage-induced DSB sites (Figure 6). We therefore conclude that Smarcal1 plays a role in NHEJ.

The molecular mechanisms underlying the severe lymphocytopenia of SIOD patients remain unclear (4,40,41). The lymphocytopenia might result primarily from a severe defect in V(D)J recombination due to the reduced efficiency of NHEJ, according to the following studies. The analysis of V(D)J recombination in peripheral T lymphocytes indicates that the size of the T-cell-antigenic receptor (TCR) repertoire is extremely small in SIOD patients (40). Moreover, the peripheral T lymphocytes of SIOD patients have severely low copy number of episomal circular DNA generated as a consequence of V(D)J recombination and contain signal joints of the T cell receptor genes (40,41). These observations support the following scenario. A moderate defect in NHEJ can cause a very strong decrease in the efficiency of T-cell development in patients, since it requires productive D-J- and V-D-recombination events in both TCRα and TCRβ chain genes in individual thymocytes. The reduced T-cell production by the thymus may be compensated by enhanced proliferation of newly generated peripheral T lymphocytes (66) in SIOD patients, leading to the quick dilution of episomal circular DNA in individual peripheral T lymphocytes. This enhanced proliferation could cause a strong replication stress in SIOD patients, due to their attenuated stabilization of replication forks. In summary, we propose that the severe lymphocytopenia of SIOD patients (4,40,41) is attributable to the significantly reduced efficiency of V(D)J recombination, together with attenuated stabilization of replication forks.

A prominent question is, how does Smarcal1 facilitate the promotion of NHEJ? We have shown that both the loss of the RPA-binding site and the inactivation of ATPase activity in Smarcal1 completely abolished the promotion of NHEJ by Smarcal1 (Figure 5E). Thus, Smarcal1 plays a role in NHEJ by physically interacting with RPA on unwound DSB ends and then facilitating their annealing. The existence of unwound single-stranded sequences at the DSB sites is supported by the presence of RPA foci in the γ-ray irradiated G_1 phase cells (67). The annealing by Smarcal1 may stabilize the interaction of DSB sites with DNA-PKcs/Ku70/Ku80, since Ku70/Ku80 associates with duplex DSB ends more stably than with DSBs carrying single-strand tails (21–24). The stabilization of DNA-PKcs/Ku70/Ku80 at DSB sites by Smarcal1 is verified by data shown in Figure 6. The following data suggest the important role of Smarcal1 in the functioning of DNA-

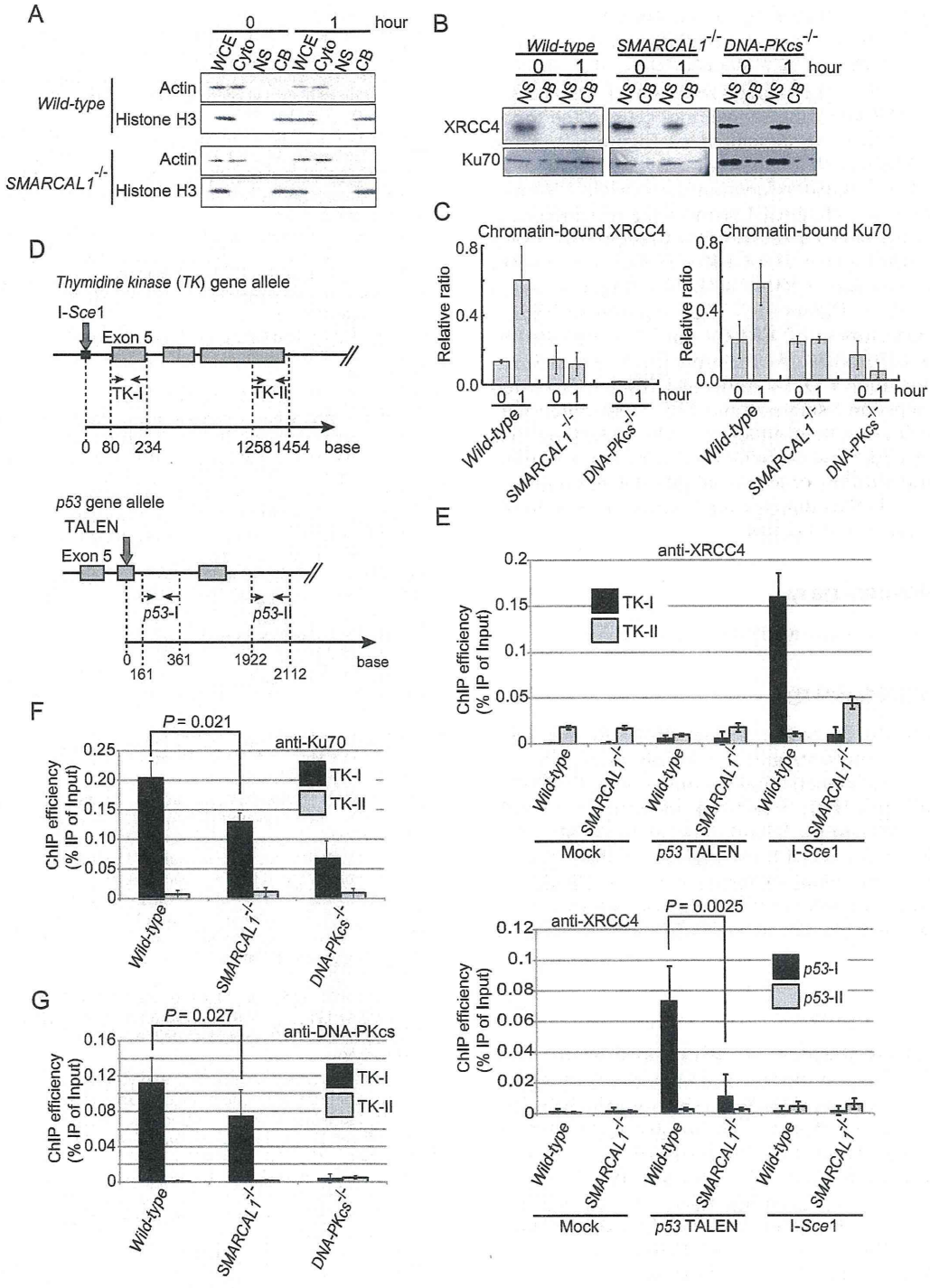

Figure 6. The loss of Smarcal1 results in compromised accumulation of Ku70, DNA-PKcs and XRCC4 at DSB sites. (**A**) Western blot data showing the validation of fractionation of the cytoplasmic (Cyto), nuclear soluble (NS) and chromatin-bound (CB) fractions isolated from the whole-cell extract (WCE). (**B**) Western blot data show the accumulation of XRCC4 (upper panel) and Ku70 (lower panel) in the chromatin-bound fraction after one-hour exposure of cells to ICRF193. (**C**) Histogram showing the quantification of XRCC4 and Ku70 in (B). The *y*-axis represents the amount of the chromatin-bound fraction relative to the total amount of the chromatin-bound fraction plus the nuclear soluble fraction. (**D**) Downward arrows represent the I-*Sce*1- (upper) and the TALEN- (lower) cutting sites in the *TK* and *p53* genes, respectively. Pairs of horizontal opposing arrows indicate the sets of primers for quantitative real-time PCR. (**E**) Histograms represent the accumulation of XRCC4 near the I-*Sce*1-induced DSB in the *TK* locus (upper panel) and near the TALEN-induced DSB at the *p53* locus (lower panel). (**F**) Histogram represents the accumulation of Ku70 near the I-*Sce*1-induced DSB in the *TK* locus. (**G**) Histogram represents the accumulation of DNA-PKcs near the I-*Sce*1-induced DSB in the *TK* locus.

PKcs. DNA-PKcs/Ku70/Ku80 also interacts with Smarcal1 *in vivo* (68,69). We here show that *DNA-PKcs*$^{-/-}$ and *SMARCAL1*$^{-/-}$ have an epistatic relationship in cellular tolerance to IR (Figure 2E). We also show that the loss of Smarcal1 inhibits the phosphorylation of DNA-PKcs at threonine 2609 following exposure of cells to the topoisomerase 2 inhibitors (Supplementary Figure S7). These observations suggest that Smarcal1 may be required for DNA-PKcs/Ku70/Ku80 to function appropriately. We also show that the loss of Smarcal1 reduces the recruitment of XRCC4 to DSB sites by several times (Figure 6). Previous studies indicate that DNA-PKcs is necessary for the stabilization of recruited XRCC4 (70,71), which is consistent with our data (Figure 6B). Thus, the effect of Smarcal1 on the recruitment of XRCC4 might be mediated by DNA-PKcs/Ku70/Ku80. We therefore propose that Smarcal1 maintains duplex DNA status at DSB ends by interacting with unwound single-strand DNA associated with RPA and facilitating their annealing. This annealing then stabilizes DNA-PKcs/Ku70/Ku80 at duplex DNA termini, which is essential for the proper accumulation and stabilization of XRCC4 at DNA damage sites. Future studies should clarify the molecular mechanism.

SUPPLEMENTARY DATA

Supplementary Data are available at NAR Online.

ACKNOWLEDGEMENTS

We are grateful to Dr Susan P. Lees-Miller for her critical reading and comments and to the Laboratory for Animal Resources and Genetic Engineering, Center for Developmental Biology (CDB), RIKEN Kobe (http://www.cdb.riken.jp/arg/cassette.html). Thanks also go to Dr Miki Shinohara for providing us with the Ligase4 antibody and to Dr Junko Murai for giving us technical advice. Finally, we wish to thank A. Noguchi and A. Kobayashi for their technical assistance and the lab members for their stimulating discussions.

FUNDING

JSPS Core-to-Core Program, A. Advanced Research Networks [to S.T.]; Grant-in-Aid for Scientific Research on Innovative Areas; Core-to-Core Program from the Ministry of Education, Culture, Sports, Science and Technology of Japan [to S.T. and H.S.]. Funding for open access charge: JSPS Core-to-Core Program, A. Advanced Research Networks; Grant-in-Aid for Scientific Research on Innovative Areas; Core-to-core Program from the Ministry of Education, Culture, Sports, Science and Technology of Japan (KAKENHI, grant number 23221005 to T.S. and H.S., 26740018 to H.S.).
Conflict of interest statement. None declared.

REFERENCES

1. Yusufzai,T., Xiangduo,K., Kyoko,Y. and Kadonaga,J.T. (2009) The annealing helicase HARP is recruited to DNA repair sites via an interaction with RPA. *Genes Dev.*, **23**, 2400–2404.
2. Yusufzai,T. and Kadonaga,J.T. (2008) HARP is an ATP-driven annealing helicase. *Science*, **322**, 748–750.
3. Bétous,R., Mason,A.C., Rambo,R.P., Bansbach,C.E., Badu-Nkansah,A., Sirbu,B.M., Eichman,B.F. and Cortez,D. (2012) SMARCAL1 catalyzes fork regression and holliday junction migration to maintain genome stability during DNA replication. *Genes Dev.*, **26**, 151–162.
4. Boerkoel,C.F., Takashima,H., John,J., Yan,J., Stankiewicz,P., Rosenbarker,L., André,J.-L., Bogdanovic,R., Burguet,A., Cockfield,S. *et al.* (2002) Mutant chromatin remodeling protein SMARCAL1 causes Schimke immuno-osseous dysplasia. *Nat. Genet.*, **30**, 215–220.
5. Deguchi,K., Clewing,J.M., Elizondo,L.I., Hirano,R., Huang,C., Choi,K., Sloan,E.A., Lücke,T., Marwedel,K.M., Powell,R.D. *et al.* (2008) Neurologic phenotype of Schimke immuno-osseous dysplasia and neurodevelopmental expression of SMARCAL1. *J. Neuropath. Exp. Neurol.*, **67**, 565–577.
6. RN,S., WA,H. and CR,K. (1971) Chondroitin-6-sulphaturia, defective cellular immunity, and nephrotic syndrome. *Lancet*, **2**, 1088–1089.
7. Spranger,J., Hinkel,G.K., Stöss,H., Thoenes,W., Wargowski,D. and Zepp,F. (1991) Schimke immuno-osseous dysplasia: a newly recognized multisystem disease. *J. Pediatr.*, **119**, 64–72.
8. Yuan,J., Ghosal,G. and Chen,J. (2009) The annealing helicase HARP protects stalled replication forks. *Genes Dev.*, **23**, 2394–2399.
9. Ciccia,A., Bredemeyer,A.L., Sowa,M.E., Terret,M.E., Jallepalli,P.V., Harper,J.W. and Elledge,S.J. (2009) The SIOD disorder protein SMARCAL1 is an RPA-interacting protein involved in replication fork restart. *Genes Dev.*, **23**, 2415–2425.
10. Bansbach,C.E., Bétous,R., Lovejoy,C.A., Glick,G.G. and Cortez,D. (2009) The annealing helicase SMARCAL1 maintains genome integrity at stalled replication forks. *Genes Dev.*, **23**, 2405–2414.
11. Jackson,S.P. (2002) Sensing and repairing DNA double-strand breaks. *Carcinogenesis*, **23**, 687–696.
12. Kanaar,R., Hoeijmakers,J.H. and van Gent,D.C. (1998) Molecular mechanisms of DNA double strand break repair. *Trends Cell Biol.*, **8**, 483–489.
13. Mehta,A. and Haber,J.E. (2014) Sources of DNA Double-Strand Breaks and Models of Recombinational DNARepair. *Cold Spring Harb. Perspect. Biol.* **6**, 1–17.
14. Kobayashi,S., Kasaishi,Y., Nakada,S., Takagi,T., Era,S., Motegi,A., Chiu,R.K., Takeda,S. and Hirota,K. (2014) Rad18 and Rnf8 facilitate homologous recombination by two distinct mechanisms, promoting Rad51 focus formation and suppressing the toxic effect of nonhomologous end joining. *Oncogene*, **0**, 1–9.
15. Maede,Y., Shimizu,H., Fukushima,T., Kogame,T., Nakamura,T., Miki,T., Takeda,S., Pommier,Y. and Murai,J. (2014) Differential and common DNA repair pathways for topoisomerase I- and II-targeted drugs in a genetic DT40 repair cell screen panel. *Mol. Cancer Therap.*, **13**, 214–220.
16. Murai,J., Huang,S.Y.N., Das,B.B., Renaud,A., Zhang,Y., Doroshow,J.H., Ji,J., Takeda,S. and Pommier,Y. (2012) Trapping of PARP1 and PARP2 by clinical PARP inhibitors. *Cancer Res.*, **72**, 5588–5599.
17. Adachi,N., Suzuki,H., Iiizumi,S. and Koyama,H. (2003) Hypersensitivity of nonhomologous DNA end-joining mutants to VP-16 and ICRF-193: implications for the repair of topoisomerase II-mediated DNA damage. *J. Biol. Chem.*, **278**, 35897–35902.
18. Boboila,C., Alt,F.W. and Schwer,B. (2012) Classical and alternative end-joining pathways for repair of lymphocyte-specific and general DNA double-strand breaks. *Adv. Immunol.*, **116**, 1–49.
19. Gellert,M. (2002) V(D)J recombination: RAG proteins, repair factors, and regulation. *Annu. Rev. Biochem.*, **71**, 101–132.
20. Verkaik,N.S., Esveldt-van Lange,R.E.E., Van Heemst,D., Brüggenwirth,H.T., Hoeijmakers,J.H.J., Zdzienicka,M.Z. and Van Gent,D.C. (2002) Different types of V(D)J recombination and end-joining defects in DNA double-strand break repair mutant mammalian cells. *Eur. J. Immunol.*, **32**, 701–709.
21. Dynan,W.S. and Yoo,S. (1998) Interaction of Ku protein and DNA-dependent protein kinase catalytic subunit with nucleic acids. *Nucleic Acids Res.*, **26**, 1551–1559.
22. Mimitou,E.P. and Symington,L.S. (2010) Ku prevents Exo1 and Sgs1-dependent resection of DNA ends in the absence of a functional MRX complex or Sae2. *EMBO J.*, **29**, 3358–3369.

23. Mimori,T. and Hardin,J.A. (1986) Mechanism of interaction between Ku protein and DNA. *J. Biol. Chem.*, **261**, 10375–10379.
24. Symington,L.S. and Gautier,J. (2011) Double-Strand Break End Resection and Repair Pathway Choice. *Ann. Rev. Genet.*, **45**, 247–271.
25. Lees-Miller,S.P., Chen,Y.R. and Anderson,C.W. (1990) Human cells contain a DNA-activated protein kinase that phosphorylates simian virus 40 T antigen, mouse p53, and the human Ku autoantigen. *Mol. Cell. Biol.*, **10**, 6472–6481.
26. Carter,T., Vancurova,I., Sun,I., Lou,W. and DeLeon,S. (1990) A DNA-activated protein kinase from HeLa cell nuclei. *Mol. Cell. Biol.*, **10**, 6460–6471.
27. Blunt,T., Gell,D., Fox,M., Taccioli,G.E., Lehmann,A.R., Jackson,S.P. and Jeggo,P.A. (1996) Identification of a nonsense mutation in the carboxyl-terminal region of DNA-dependent protein kinase catalytic subunit in the scid mouse. *Proc. Natl. Acad. Sci. U.S.A.*, **93**, 10285–10290.
28. Chan,D.W., Chen,B.P.-C., Prithivirajsingh,S., Kurimasa,A., Story,M.D., Qin,J. and Chen,D.J. (2002) Autophosphorylation of the DNA-dependent protein kinase catalytic subunit is required for rejoining of DNA double-strand breaks. *Genes Dev.*, **16**, 2333–2338.
29. Cui,X., Yu,Y., Gupta,S., Cho,Y.-M., Lees-Miller,S.P. and Meek,K. (2005) Autophosphorylation of DNA-dependent protein kinase regulates DNA end processing and may also alter double-strand break repair pathway choice. *Mol. Cell. Biol.*, **25**, 10842–10852.
30. Ma,Y., Pannicke,U., Lu,H., Niewolik,D., Schwarz,K. and Lieber,M.R. (2005) The DNA-dependent protein kinase catalytic subunit phosphorylation sites in human Artemis. *J. Biol. Chem.*, **280**, 33839–33846.
31. Reddy,Y.V.R., Ding,Q., Lees-Miller,S.P., Meek,K. and Ramsden,D.A. (2004) Non-homologous end joining requires that the DNA-PK complex undergo an autophosphorylation-dependent rearrangement at DNA ends. *J. Biol. Chem.*, **279**, 39408–39413.
32. Ahnesorg,P., Smith,P. and Jackson,S.P. (2006) XLF interacts with the XRCC4-DNA Ligase IV complex to promote DNA nonhomologous end-joining. *Cell*, **124**, 301–313.
33. Buck,D., Malivert,L., De Chasseval,R., Barraud,A., Fondanèche,M.C., Sanal,O., Plebani,A., Stéphan,J.L., Hufnagel,M., Le Deist,F. *et al.* (2006) Cernunnos, a novel nonhomologous end-joining factor, is mutated in human immunodeficiency with microcephaly. *Cell*, **124**, 287–299.
34. Critchlow,S.E., Bowater,R.P. and Jackson,S.P. (1997) Mammalian DNA double-strand break repair protein XRCC4 interacts with DNA ligase IV. *Curr. Biol.*, **7**, 588–598.
35. Grawunder,U., Wilm,M., Wu,X., Kulesza,P., Wilson,T.E., Mann,M. and Lieber,M.R. (1997) Activity of DNA ligase IV stimulated by complex formation with XRCC4 protein in mammalian cells. *Nature*, **388**, 492–495.
36. Lieber,M.R. (2010) NHEJ and its backup pathways in chromosomal translocations. *Nat. Struct. Mol. Biol.*, **17**, 393–395.
37. Simsek,D. and Jasin,M. (2010) Alternative end-joining is suppressed by the canonical NHEJ component Xrcc4-ligase IV during chromosomal translocation formation. *Nat. Struct. Mol. Biol.*, **17**, 410–416.
38. Buerstedde,J.M. and Takeda,S. (1991) Increased ratio of targeted to random integration after transfection of chicken B cell lines. *Cell*, **67**, 179–188.
39. Takashima,Y., Sakuraba,M., Koizumi,T., Sakamoto,H., Hayashi,M. and Honma,M. (2009) Dependence of DNA double strand break repair pathways on cell cycle phase in human lymphoblastoid cells. *Environ. Mol. Mutagen.*, **50**, 815–822.
40. Lev,A., Amariglio,N., Levy,Y., Spirer,Z., Anikster,Y., Rechavi,G., Dekel,B. and Somech,R. (2009) Molecular assessment of thymic capacities in patients with Schimke immuno-osseous dysplasia. *Clin. Immunol.*, **133**, 375–381.
41. Simon,A.J., Lev,A., Jeison,M., Borochowitz,Z.U., Korn,D., Lerenthal,Y. and Somech,R. (2014) Novel SMARCAL1 bi-allelic mutations associated with a chromosomal breakage phenotype in a severe SIOD patient. *J. Clin. Immunol.*, **34**, 76–83.
42. Sonoda,E., Sasaki,M.S., Buerstedde,J.M., Bezzubova,O., Shinohara,A., Ogawa,H., Takata,M., Yamaguchi-Iwai,Y. and Takeda,S. (1998) Rad51-deficient vertebrate cells accumulate chromosomal breaks prior to cell death. *EMBO J.*, **17**, 598–608.
43. Cermak,T., Doyle,E. and Christian,M. (2011) Efficient design and assembly of custom TALEN and other TAL effector-based constructs for DNA targeting. *Nucleic Acids Res.*, **39**, e82.
44. Sakuma,T., Ochiai,H., Kaneko,T., Mashimo,T., Tokumasu,D., Sakane,Y., Suzuki,K.-i., Miyamoto,T., Sakamoto,N., Matsuura,S. *et al.* (2013) Repeating pattern of non-RVD variations in DNA-binding modules enhances TALEN activity. *Sci. Rep.*, **3**, 3379.
45. Ran,F.A., Hsu,P.D., Lin,C.Y., Gootenberg,J.S., Konermann,S., Trevino,A.E., Scott,D.A., Inoue,A., Matoba,S., Zhang,Y. *et al.* (2013) Double nicking by RNA-guided CRISPR cas9 for enhanced genome editing specificity. *Cell*, **154**, 1380–1389.
46. Qing,Y., Yamazoe,M., Hirota,K., Dejsuphong,D., Sakai,W., Yamamoto,K.N., Bishop,D.K., Wu,X. and Takeda,S. (2011) The epistatic relationship between BRCA2 and the other RAD51 mediators in homologous recombination. *PLoS Genet.*, **7**, 1002148.
47. Zhao,G.Y., Sonoda,E., Barber,L.J., Oka,H., Murakawa,Y., Yamada,K., Ikura,T., Wang,X., Kobayashi,M., Yamamoto,K. *et al.* (2007) A critical role for the ubiquitin-conjugating enzyme Ubc13 in initiating homologous recombination. *Mol. Cell*, **25**, 663–675.
48. Hesse,J.E., Lieber,M.R., Gellert,M. and Mizuuchi,K. (1987) Extrachromosomal DNA substrates in pre-B cells undergo inversion or deletion at immunoglobulin V-(D)-J joining signals. *Cell*, **49**, 775–783.
49. Arad,U. (1998) Modified Hirt procedure for rapid purification of extrachromosomal DNA from mammalian cells. *Biotechniques*, **24**, 760–762.
50. Taccioli,G.E., Rathbun,G., Oltz,E., Stamato,T., Jeggo,P.A. and Alt,F.W. (1993) Impairment of V(D)J recombination in double-strand break repair mutants. *Science*, **260**, 207–210.
51. Honma,M., Izumi,M., Sakuraba,M., Tadokoro,S., Sakamoto,H., Wang,W., Yatagai,F. and Hayashi,M. (2003) Deletion, rearrangement, and gene conversion; genetic consequences of chromosomal double-strand breaks in human cells. *Environ. Mol. Mutagen.*, **42**, 288–298.
52. Honma,M., Sakuraba,M., Koizumi,T., Takashima,Y., Sakamoto,H. and Hayashi,M. (2007) Non-homologous end-joining for repairing I-SceI-induced DNA double strand breaks in human cells. *DNA Repair*, **6**, 781–788.
53. Sasanuma,H., Murakami,H., Fukuda,T., Shibata,T., Nicolas,A. and Ohta,K. (2007) Meiotic association between Spo11 regulated by Rec102, Rec104 and Rec114. *Nucleic Acids Res.*, **35**, 1119–1133.
54. Postow,L., Woo,E.M., Chait,B.T. and Funabiki,H. (2009) Identification of SMARCAL1 as a component of the DNA damage response. *J. Biol. Chem.*, **284**, 35951–35961.
55. Takata,M., Sasaki,M.S., Tachiiri,S., Fukushima,T., Sonoda,E., Schild,D., Thompson,L.H. and Takeda,S. (2001) Chromosome instability and defective recombinational repair in knockout mutants of the five Rad51 paralogs. *Mol. Cell. Biol.*, **21**, 2858–2866.
56. Kirkland,D., Pfuhler,S., Tweats,D., Aardema,M., Corvi,R., Darroudi,F., Elhajouji,A., Glatt,H., Hastwell,P., Hayashi,M. *et al.* (2007) How to reduce false positive results when undertaking in vitro genotoxicity testing and thus avoid unnecessary follow-up animal tests: Report of an ECVAM Workshop. *Mut. Res.*, **628**, 31–55.
57. Zhang,L.S., Honma,M., Hayashi,M., Suzuki,T., Matsuoka,A. and Sofuni,T. (1995) A comparative study of TK6 human lymphoblastoid and L5178Y mouse lymphoma cell lines in the in vitro micronucleus test. *Mut. Res.*, **347**, 105–115.
58. Oettinger,M.A., Schatz,D.G., Gorka,C. and Baltimore,D. (1990) RAG-1 and RAG-2, adjacent genes that synergistically activate V(D)J recombination. *Science*, **248**, 1517–1523.
59. Schatz,D.G., Oettinger,M.A. and Baltimore,D. (1989) The V(D)J recombination activating gene, RAG-1. *Cell*, **59**, 1035–1048.
60. Schatz,D.G. (1997) V(D)J recombination moves in vitro. *Semin. Immunol.*, **9**, 149–159.
61. Frank,K.M., Sekiguchi,J.M., Seidl,K.J., Swat,W., Rathbun,G.A., Cheng,H.L., Davidson,L., Kangaloo,L. and Alt,F.W. (1998) Late embryonic lethality and impaired V(D)J recombination in mice lacking DNA ligase IV. *Nature*, **396**, 173–177.
62. Grawunder,U., Zimmer,D., Fugmann,S., Schwarz,K. and Lieber,M.R. (1998) DNA ligase IV is essential for V(D)J recombination and DNA double-strand break repair in human precursor lymphocytes. *Mol. Cell*, **2**, 477–484.
63. Chen,B.P.C., Uematsu,N., Kobayashi,J., Lerenthal,Y., Krempler,A., Yajima,H., Löbrich,M., Shiloh,Y. and Chen,D.J. (2007) Ataxia

telangiectasia mutated (ATM) is essential for DNA-PKcs phosphorylations at the Thr-2609 cluster upon DNA double strand break. *J. Biol. Chem.*, **282**, 6582–6587.
64. Ding,Q., Reddy,Y.V., Wang,W., Woods,T., Douglas,P., Ramsden,D.A., Lees-Miller,S.P. and Meek,K. (2003) Autophosphorylation of the catalytic subunit of the DNA-dependent protein kinase is required for efficient end processing during DNA double-strand break repair. *Mol. Cell. Biol.*, **23**, 5836–5848.
65. Bansbach,C.E., Boerkoel,C.F. and Cortez,D. (2010) SMARCAL1 and replication stress: An explanationfor SIOD? *Nucleus*, **1**, 245–248.
66. Takeda,S., Rodewald,H.R., Arakawa,H., Bluethmann,H. and Shimizu,T. (1996) MHC class II molecules are not required for survival of newly generated CD4+ T cells, but affect their long-term life span. *Immunity*, **5**, 217–228.
67. Barton,O., Naumann,S.C., Diemer-Biehs,R., Kunzel,J., Steinlage,M., Conrad,S., Makharashvili,N., Wang,J., Feng,L., Lopez,B.S. *et al.* (2014) Polo-like kinase 3 regulates CtIP during DNA double-strand break repair in G1. *J. Cell Biol.*, **206**, 877–894.
68. Betous,R., Glick,G.G., Zhao,R. and Cortez,D. (2013) Identification and characterization of SMARCAL1 protein complexes. *PloS One*, **8**, e63149.
69. Quan,J. and Yusufzai,T. (2014) HARP preferentially co-purifies with RPA bound to DNA-PK and blocks RPA phosphorylation. *Epigenetics*, **9**, 693–697.
70. Drouet,J., Delteil,C., Lefrancois,J., Concannon,P., Salles,B. and Calsou,P. (2005) DNA-dependent protein kinase and XRCC4-DNAligase IV mobilization in the cell in response to DNA double strand breaks. *J. Biol. Chem.*, **280**, 7060–7069.
71. Yano,K.I. and Chen,D.J. (2008) Live cell imaging of XLF and XRCC4 reveals anovel view of protein assembly in the non-homologous end-joining pathway. *Cell Cycle*, **7**, 1321–1325.

PLOS | ONE

RESEARCH ARTICLE

Xeroderma Pigmentosum Group A Suppresses Mutagenesis Caused by Clustered Oxidative DNA Adducts in the Human Genome

Akira Sassa*, Nagisa Kamoshita, Yuki Kanemaru¤, Masamitsu Honma, Manabu Yasui*

Division of Genetics and Mutagenesis, National Institute of Health Sciences, Setagaya-ku, Tokyo, Japan

¤ Current address: Division of Toxicology, Department of Pharmacology, Toxicology and Therapeutics, Showa University School of Pharmacy, Shinagawa-ku, Tokyo, Japan
* m-yasui@nihs.go.jp (MY); a-sassa@nihs.go.jp (AS)

Citation: Sassa A, Kamoshita N, Kanemaru Y, Honma M, Yasui M (2015) Xeroderma Pigmentosum Group A Suppresses Mutagenesis Caused by Clustered Oxidative DNA Adducts in the Human Genome. PLoS ONE 10(11): e0142218. doi:10.1371/journal.pone.0142218

Editor: Komaraiah Palle, University of South Alabama Mitchell Cancer Institute, UNITED STATES

Received: August 26, 2015

Accepted: October 19, 2015

Published: November 11, 2015

Data Availability Statement: All relevant data are within the paper and its Supporting Information files.

Funding: The work was supported by the following: 25281022, Grant-in-Aid for Scientific Research (B) from the Ministry of Education, Culture, Sports, Science and Technology in Japan, MY, http://www.mext.go.jp/english/; and H27-food-general-002, Grant-in-Aid for Health Science Foundation from the Ministry of Health, Welfare and Labor in Japan, MH, http://www.mhlw.go.jp/english/. The funders had no role in study design, data collection and analysis, decision to publish, or preparation of the manuscript.

Abstract

Clustered DNA damage is defined as multiple sites of DNA damage within one or two helical turns of the duplex DNA. This complex damage is often formed by exposure of the genome to ionizing radiation and is difficult to repair. The mutagenic potential and repair mechanisms of clustered DNA damage in human cells remain to be elucidated. In this study, we investigated the involvement of nucleotide excision repair (NER) in clustered oxidative DNA adducts. To identify the *in vivo* protective roles of NER, we established a human cell line lacking the NER gene xeroderma pigmentosum group A (*XPA*). *XPA* knockout (KO) cells were generated from TSCER122 cells derived from the human lymphoblastoid TK6 cell line. To analyze the mutagenic events in DNA adducts *in vivo*, we previously employed a system of tracing DNA adducts in the targeted mutagenesis (TATAM), in which DNA adducts were site-specifically introduced into intron 4 of thymidine kinase genes. Using the TATAM system, one or two tandem 7,8-dihydro-8-oxoguanine (8-oxoG) adducts were introduced into the genomes of TSCER122 or *XPA* KO cells. In *XPA* KO cells, the proportion of mutants induced by a single 8-oxoG (7.6%) was comparable with that in TSCER122 cells (8.1%). In contrast, the lack of XPA significantly enhanced the mutant proportion of tandem 8-oxoG in the transcribed strand (12%) compared with that in TSCER122 cells (7.4%) but not in the non-transcribed strand (12% and 11% in *XPA* KO and TSCER122 cells, respectively). By sequencing the tandem 8-oxoG-integrated loci in the transcribed strand, we found that the proportion of tandem mutations was markedly increased in *XPA* KO cells. These results indicate that NER is involved in repairing clustered DNA adducts in the transcribed strand *in vivo*.

Introduction

Genomic DNA is constantly exposed to both exogenous and endogenous genotoxic agents. Among them, ionizing radiation (IR) induces various DNA adducts in the genome because of

Competing Interests: The authors have declared that no competing interests exist.

its ability to produce reactive oxygen species in cells. Moreover, IR induces clustered DNA damage, which is defined as multiple DNA damage sites [oxidized DNA adducts, apurinic/apyrimidinic (AP) sites, or strand breaks] within one or two helical turns of the duplex DNA. Non-double-strand break (DSB) clustered DNA damage comprises 70%–80% of the complex DNA damage induced by IR, whereas DSB accounts for 20%–30% [1, 2]. Clustered DNA damage is considered to be more difficult to repair than a single DNA damage site. Unrepaired damage contributes to mutagenesis, cancer development, and disease [3].

7,8-Dihydro-8-oxoguanine (8-oxoG) is one of the major oxidative DNA adducts induced by IR. Because of the altered hydrogen-bonding potential, 8-oxoG can pair with an adenine during replication [4] and cause G·C to T·A transversion mutations. 8-OxoG is primarily repaired by the base excision repair (BER) pathway [5]. In mammalian cells, 8-oxoG paired with cytosine is readily repaired by 8-oxoguanine DNA glycosylase (OGG1)-initiated BER [6]. Furthermore, repair can occur via another BER pathway in which the human *MutY* homolog (MYH) removes an adenine from the 8-oxoGA mispair [7]. However, it is more challenging to repair 8-oxoG in clustered DNA damage sites via BER.

Numerous studies have investigated BER retardation at clustered DNA damage sites that results in enhanced genomic instability. Different types of damage (a thymine glycol, an AP site, a single-strand break, or a mismatched base-pair) adjacent to 8-oxoG strongly inhibits 8-oxoG excision by OGG1 [8–10]. When two 8-oxoG are located in tandem nucleotides on the same strand, the repair of these adducts is also delayed [11]. DNA damage in close opposition to an 8-oxoG also inhibits 8-oxoG repair [12–14]. The biological relevance of these clustered damages in DNA has been extensively investigated in both *Escherichia coli* and yeast [15–24]. However, although several studies have examined the mutagenic events of clustered oxidative damage to episomal DNA in mammalian cells [25, 26], these repair mechanisms in the human genome are still not well understood.

A few previous reports have indicated that nucleotide excision repair (NER), which repairs bulky DNA adducts (such as cyclobutane pyrimidine dimers), is involved in the removal of oxidative DNA adducts. An *in vitro* study demonstrated that NER recognizes 8-oxoG in oligonucleotides [27]. A high-sensitivity method that combined single-cell gel electrophoresis with fluorescence *in situ* hybridization also revealed 8-oxoG removal from the transcribed strand (TS) of DNA by transcription-coupled NER [28]. On the basis of these studies, we posed the following question: what role does NER play in the suppression of mutagenesis induced by a single and/or clustered 8-oxoG formed in the genome?

Here we established a human cell line lacking xeroderma pigmentosum complementation group A (*XPA*), a gene essential for NER on both TS and the non-transcribed strand (NTS) [29]. We previously developed a unique system for tracing DNA adducts in targeting mutagenesis (TATAM) by introducing a DNA adduct site specifically into intron 4 of the thymidine kinase (*TK*) gene in human lymphoblastoid cells [30]. Using the TATAM system, either one or two tandemly located 8-oxoG were introduced into the genome of the wild-type or *XPA* knockout (KO) cells for analysis of the mutagenic potential of adducts. Our findings indicate that NER is a possible repair mechanism of clustered oxidative DNA adducts particularly in TS of the human genome.

Materials and Methods

Cell culture

Human lymphoblastoid TSCER122 cells, which were derived from TK6 cells [31], have been previously described [30]. Cells were cultured in RPMI 1640 (Nacalai Tesque) with 10% heat-